Saudi Journal of Biological Sciences 28 (2021) 1093–1099

Contents lists available at ScienceDirect

Saudi Journal of Biological Sciences

journal homepage: www.sciencedirect.com

Original article

Silver nanoparticles biosynthesis using Saussurea costus root aqueous extract and catalytic degradation efficacy of safranin dye

Abeer R.M. Abd El-Aziz [a,*], Annadurai Gurusamy [b], Monira R. Alothman [a], Shereen M. Shehata [c], Sameh M. Hisham [a], Afnan A. Alobathani [a]

[a] Botany and Microbiology, Department, College of Science, King Saud University, Riyadh, Saudi Arabia
[b] Manonmaniam Sundaranar University, MSUNIV, Sri Paramakalyani Centre for Environmental Sciences (SPKCES) at Alwarkurichi, India
[c] Pharmaceutical Chemistry Depart, College of Pharmacy, King Saud University, Riyadh, Saudi Arabia

ARTICLE INFO

Article history:
Received 18 October 2020
Revised 5 November 2020
Accepted 8 November 2020
Available online 19 November 2020

Keywords:
Silver nano-particles
Saussurea costus root extract
Degradation
Safranin dye

ABSTRACT

Nanobiotechnology is a fast growing field in which instruments are created by nano size particles of approximately 1 to 100 nm (1 to 100 nm) of the scale of nanometers. Nanoparticles today have potential implications for life sciences and human health applications. In this research, silver nanoparticles (AgNPs) were successfully synthesized using Saussurea costus root aqueous extract and AgNPs have been characterized by the use of UV–Vis, Scanning Electron Microscopes (SEM), and Electromicroscopy of transmission (TEM) and Energy Dispersive X-ray Spectroscopy (EDXs). The highest number of particles are in the 5 to 15 nm range. AgNPs have been added in saffron dye solution for degradation dye biosynthesizing, and product analysis using UV/vision spectrophotometer, FTIR and HPLC has been performed. Green-summed AgNPs effectively degraded the color, with UV/VIS spectrophotometers, around 84.6 percent at 72 h of exposure time. The decrease in tested dye and presence of multiple new highs in the samples treated with different retention times (Rt) 2.30, 6.10 and 12.24 min, is positive for the biodegradation compared to the untreated dye with single high at 10.31 min, respectively. This green chemistry is very advantageous for AgNPs biosynthesis, for example, cost-effectiveness and usability for medicinal, pharmaceutical and extensive industrial applications. Furthermore, the bio-recovery unit for plant extracts provides a greater ease of handling, compared to micro-organisms.

1. Introduction

Various toxic contaminants are created and considered harmful to humans and the environment through industrial production. Synthetic dyes, which are difficult to extract by natural methods, are the world's largest chemical category. Therefore, color elimination is important for human security and ecosystem protection. Much attention has been paid in recent years to investigating the degradation of dye contaminants using several methods, such as photocatalytic degradation (Liu and Zhao, 2000; Vinodgopal and Kamat, 1995) oxidative processes (Hammami et al., 2007), biodegradation (Cariasa et al., 2008; Jadhava et al., 2008), but these methods needed special conditions and time consuming, so it was important to look for an easy and simple method for degradation. Nanoparticles have peculiar chemical, mechanical, magnetic and visual properties because of their small size and large surface area (Logunov et al., 1997; Hodak et al., 1998). Nanoparticles biodegradation is an environmentally friendly and cost-effective option. The convergence between the biotechnological and nanotechnology technologies leads to the biosynthesis of the nanoparticles as emerging bio-nanotechnologies. The use of biotechnology such as plant extracts and microorganisms has become an alternative to physical and chemical processes through environmentally friendly methodologies and ecological syntheses (Gardea-Torresdey et al., 2003). Furthermore, using plant extracts for nanoparticles synthesis could be advantageous over microorganisms because of numerous factors such as easy handling, cell maintenance obstruction, a large number of plant extracts can be obtained quickly, but the plant material is the best reduction agent for obtaining excellent nanoparticle size and shape (Saxena et al., 2012). Nanoparticles

* Corresponding author.
E-mail address: aabdelaziz@ksu.edu.sa (A.R.M. Abd El-Aziz).
Peer review under responsibility of King Saud University.

Production and hosting by Elsevier

https://doi.org/10.1016/j.sjbs.2020.11.036
1319-562X/

without contamination and having a given size and morphology can result from Biosynthesis. Furthermore, by biosynthetic methods, specified sizes and morphology of nanoparticles can be generated better than physicochemical (Ravindran and Chandran, 2013). The plant produces a complex enzyme and numerous chemicals such as polyphenols, sterols, flavonoids, triterpenes and proteins that can create metallic nanoparticles, and reducing agents such as sugar (fructose and glucose) (Bonnia et al., 2016). Lipschitz, syn Saussuraa Lappa C.B. *Saussurea costus* (Falc.) Clarke family Asteraciae, which comprises around 1000 genera, is known in English as costus and has different names for slang in India, as in the case of the Kur (Bengal), the Kut (Gujrati), the Sepuddy (Malayalam), the Kot (Punjabi), and the Postkhai (Punjabi), the Kushta (Sanskrit). Saussurea costus (S. costus) is a famous and important medicinal plant widely used for the treatment of various conditions in medicine; traditionally S. Costs are added as an antiseptic, sedative, carminative, and bronchodilating agent.

In this survey, we recorded silver nanoparticles with Saussurea costus radical extract biosynthesis, and synthesized AgNPs were used for environmental degradation of the application of dye contaminants.

2. Materials and methods

2.1. Preparation of Saussurea costus root aqueous extract

Dried S. Dry. Costus from Al-Riyadh local market. The extract has been prepared using the Whatman filter (No. 1) by boiling 10 g of costumes in deionized water and boiling it for about 15 min. The extract was centrifuged for 15 min at 5000 rpm after collecting the overflowing material.

2.2. AgNPs biosynthesis

A shaker with a steady rotation of 27 ± 2° C at room temperature for 24 h was mixed in 10 mL costal aquatic extract with 100 mL of silver nitrate (1 mM) solution. Silver nitrate solution of 1 mM was used as monitor, without extract.

2.3. Silver nanoparticles characterization

Some techniques have been used to classify synthesized silver nanoparticles:

2.3.1. Spectroscopy of UV/vis

The UV–Vis (Model Victoria, Australia) spectrophotometer is used for characterization of wavelengths between 200 and 1000 nm of synthesis of silver nanoparticles. By the forming of surface Plasmon Resonance Peak (~420 nm) with UV/VIS spectroscopy, the reduction of $AgNO_3$ in AGNPs by the addition of aqueous seed extract was identified.

2.3.2. Scanning electron microscopy

The morphology of AgNPs was studied using SEM a QUANTA 250 instrument fitted with an EDS. The dried silver powder was placed on a copper-coated carbon grid. EDS research was conducted to assess the atomic composition of AgNPs.

2.3.3. Transmission electron microscopy

A transmission electron microscopy (JEM 1400 plus model, with an acceleration voltage of 100 kv) was used for the morphology, sizes, and agglomeration of silver Nanoparticles. Computer Picture J was used to evaluate images and to measure the particle size.

2.4. Preparation of solution of saffron dye stock

A 1000 mL of twin distilled water used as a supplying solution has been added to 10 mg of Safranine-O (3,7-diamino-2,8-dime thyl-5-phenylphenazinium chloride) colorant (merck, Germany).

2.4.1. Safranin dye catalytic degradation

In 100 mL of Safranine dye solution, approximately 10 mg of biosynthesized silver nanoparticles were added. A control was also maintained without addition of silver nanoparticles, then their action suspension was mixed well by being magnetic stirred for 72 h. at fixed time intervals.

2.5. Biological analyzes of saffron dye

2.5.1. UV–Vis spectrophotometer

The dye concentration was measured with an absorbance value of 520 nm during degradation. Dye percentage has been determined as follows (Abd El-Aziz et al., 2018): The following formula: $\%Decolourization = 1 - \frac{A_t}{A_0} \times 100$ where A0 is the initial absorbance and at corresponds to the maximum absorbance t at the wavelength.

2.5.2. Fourier transformed infrared spectroscopy

Biodegradation of saffron thing was measured before and after degradation by analyzing peak FTIR profiles in degraded color samples. The FTIR-spectrometer was developed with a 4 cm^{-1} wave-size resolution of 400–4000 cm^{-1} on the Nicolet 6700 spectrometer (Thermo Electron Company, USA).

2.5.3. HPLC review

The high-performance liquid chromatography (Model PerkinElmer series 200 UV/VIS) was used to track degraded intermediates using a 300 mm internal diameter column C18, 3.9 mm internal column, 4 μm with mobile methanol phases (80 percent) and 20 percent deionized water. The HPLC has a 365 nm arousal and 430 wavelengths of emission UV detectors and fluorescence). Sample filtration was carried out using a membrane of 0.22 μl and then analyzed at a flow rate of 1 mL/min.

3. Results

3.1. Characterization of silver nanoparticles

The S add-on. The price (Fig. 1) is shown in. S. Costal ion solution aqueous root (10–3 mol/L), which reflected the production of AgNPs, turning color of the solution into greenish-brown.

3.1.1. Spectrometry of UV–Vis

The presence of AgNPs in the solution was confirmed by UV–Vis spectrophotometry (Fig. 2).

3.1.2. SEM

The image of SEM shows the biosynthesized silver nanoparticles using S. Costus root extracts. Since small nanoparticles were aggregated (Fig. 3), some of the large nanoparticles were associated with spherical shape of high-agglomeration nanoparticles. Some particles were scattered while others were mixed, possibly because of the longer time after the synthesis for SEM experiment.

In the region of silver 3 keV, the EDS spectrum (Fig. 3b) shows a clear signal supporting the creation of nanosilver and its basic nature.

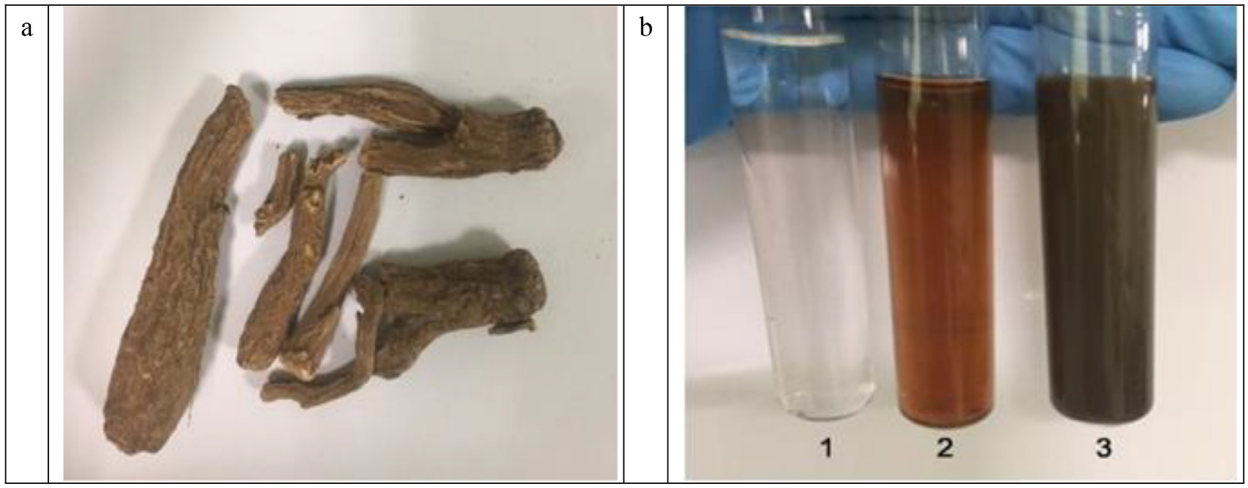

Fig. 1. Dried root of *S. costus* (a), *S. costus* root aqueous extract (b) (1), aqueous solution of 10^{-3} mmol/L $AgCl_3$ (2) and aqueous solution of 10–3 mmol/L $AgCl_3$ with *S. costus* (3).

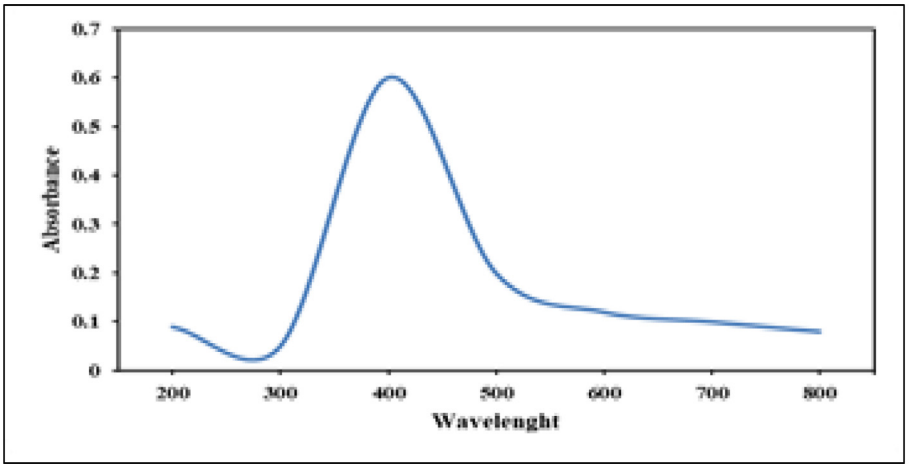

Fig. 2. UV–Vis absorbance bands at 533 nm for AuNPs forms *S. costus* root aqueous extract.

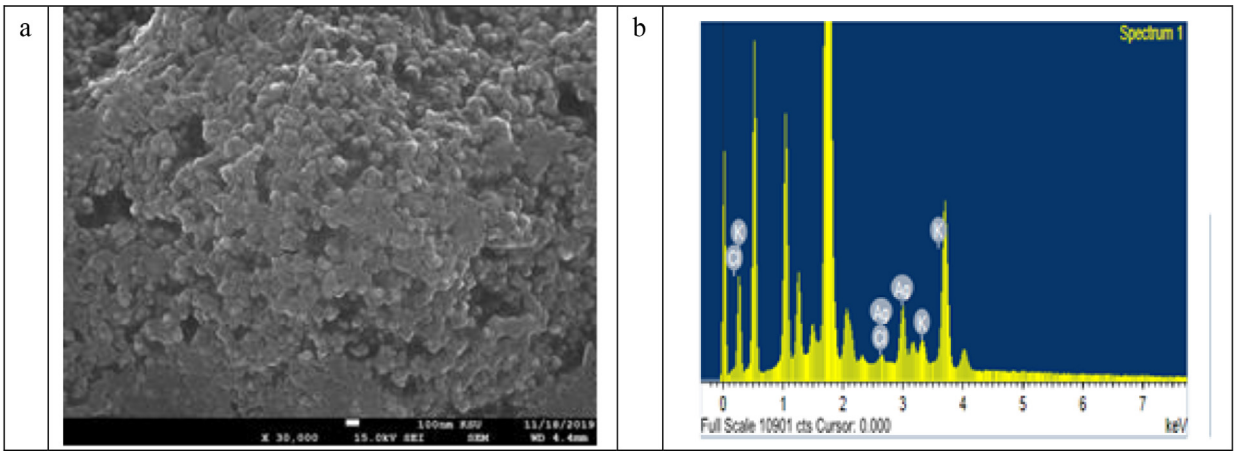

Fig. 3. SEM images of AgNPs (a) and EDS spectrum of AgNPs synthesized using *S. costus* root aqueous extract (b).

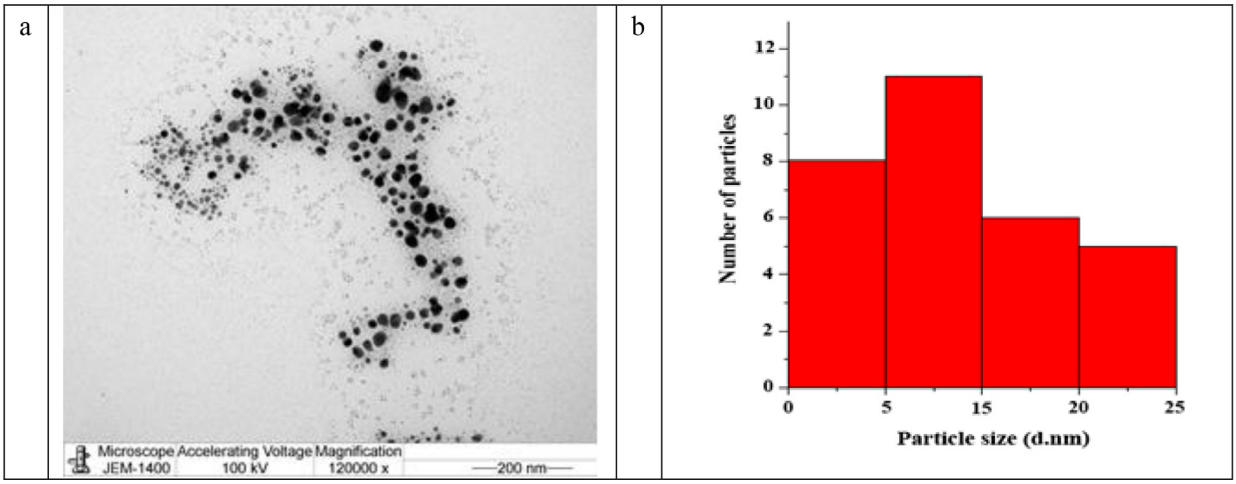

Fig. 4. TEM image of the AgNPs forms using *S. costus* root aqueous extract of 120,000× (a) and the histogram of the particle size distribution of the AgNPs (b).

3.1.3. TEM

The structure and form of TEM nanoparticles determined (Fig. 4a) suggested the spherical and monodispersed particles without major agglomeration (shapes distributed evenly). The Particle Size histogram (Fig. 4b) displays a number of particle sizes from 5 nm to 25 nm. The maximum particle distribution is between 5 and 15 nm.

3.2. Catalytic color loss

3.2.1. Spectrometry of UV–Vis

Dye degradation of saffron was performed in the visible region in the presence of Ag NPs at another time. The absorption spectrum showed decreased safranine dye peaks at various times in Fig. 6. Fig. 3. Initially, with the increase in exposure time, absorption peaks of safranin dye were steadily lowered at 5 20 nm and the degradation of safranina dye was seen. The overall absorption of safranine dye has been reduced, while the absorption range of AgNPs has been increased to 420 nm. The catalytic degradation of the dye was achieved when the absorption peak approached the base line and the peak increased for Ag NPs.

The data collected in (Table 1) and (Fig. 7) indicate the percentage degradation of saffron dye by AgNPs; the information received shows that safranine degradation has increased over time.

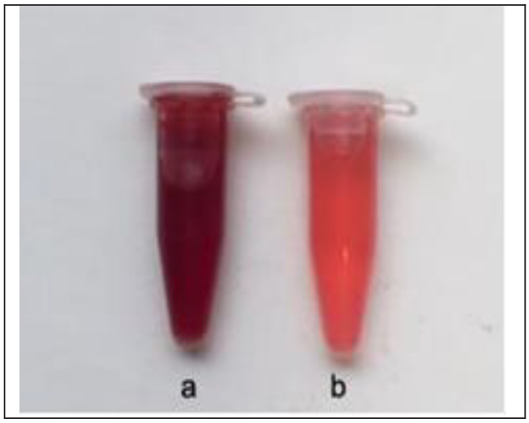

Fig. 5. Visual observation of color change from red to colorless indicates degradation of safranin dye at different time intervals (a) initial, (b) and 72 h.

3.2.2. FTIR

Fig. 8 displays the pure dye FTIR spectrum and AgNPs degraded dye. FTIR analysis was performed on synthesized AgNPs to detect nanoparticles in the range 400–4000 cm^{-1} with their related bioactive compounds. At 2205, 75 cm^{-1}, 2181, 63 and 2046, 11 cm^{-1}, the 3-band absorption of the aromatic C – C in-ring stretching in the teeth absolutely waned after AgNP treatment. Degrading products are due to the appearance of a new absorption band at 1998.52 cm^{-1}. Moreover, the 3280.19 cm^{1} peaks of safranin color were moved to 3283.53 cm^{-1}, 2157.69 m^{-1} shifting to 2158.04 cm^{1}, 2014.84 cm^{-1}, 2015.62 cm^{-1}, 163521636.48 cm^{-1}, shows a dye/AgNPs deterioration. Four peaks have been moved to another wave numbers.

3.2.3. Analysis of HPLC

HPLC tracked the degraded intermediates. During the degradation of safranin with AgNPs at retention times 2.30, 6.10 and 12.24 min, an examination of untreated safranine dye (Fig. 9a) showed single maximum retention time 10.31 min while (Fig. 9b) four distinct intermediates degraded products appeared.

4. Discussion

Changes in color suggest that the proteins present and the bioactive components are decreased by the silver ions in the herbal extract (Mahapatra et al., 2018). The surface Plasm Resonance of Ag NPs (Al-Mashhedy and Al-Kawaz, 2016) has caused the color formation. Several researchers (Govindaraju et al., 2010) found similar results in the use of Solanium torvum leaf extract to synthesize Ag np (Rao & Savithramma 2011) when they observed the color shift to brownish yellow. The results are similar. The Svensonia hyderabadensis solution for the silver ion complex also has been reported to start changing color from yellow to dark brown as silver ions were reduced (Chen et al., 2004). The degree of color formation in the reaction mix of various plants, such as Helianthus annuus, Basella alba and Saccharum officinarum (Al-Othman et al., 2017) demonstrated that, once $AgNO_3$ was added to the grenade pomegranate extract (Alothman, and Abd-El-Aziz, 2019) the mixture's color changed between gel and dark brow. It was also reported that the color changed to dark brown with growing intensity following $AgNO_3$ applied to banana, fish, orange, mandarin and kivi peels.

The results of UV–Vis spectrophotometry show a high 420 nm peak, suggesting the formation of AgNPs. The clear shift was within 72 h (Vanaja et al., 2014; Abd El-Aziz et al., 2018). The findings of

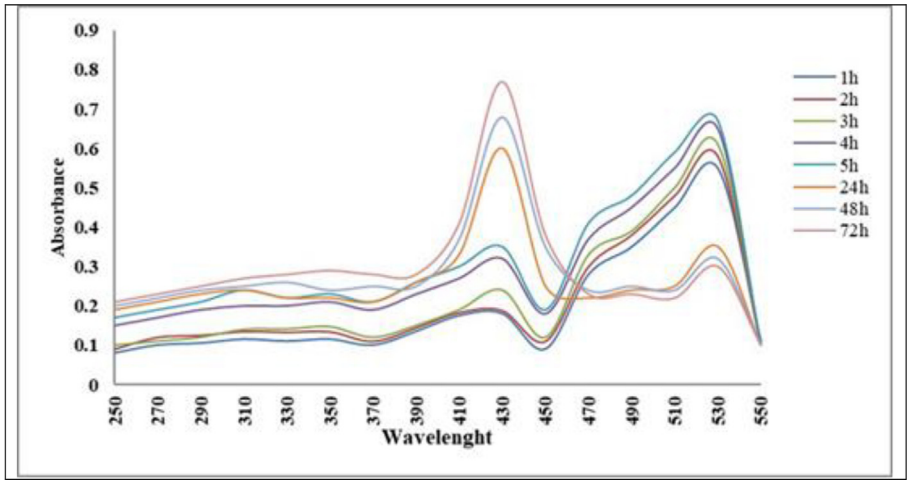

Fig. 6. Absorption spectra of safranin dye treated with 10 mg/L of AgNPs synthesized using *S. costus at* different time points.

Table 1
Degradation of safranin dye (%) by synthesized silver nanoparticles (10 mg).

Exposure time (h)	Amount of degradation of dye (%)
1	2.3 ± 0.32
2	5.1 ± 0.28
3	8.9 ± 0.23
4	10.2 ± 0.37
5	13.1 ± 0.29
24	35.3 ± 0.37
48	62.3 ± 0.27
72	84.6 ± 0.42

± Standard deviation.

SEM correspond to previous reports (Abd El-Aziz et al., 2018). The activation of the Plasmon resonance surface Ag NPs has provided this signal. In the range that corresponds to other elements, impurities from bio-extract molecules such as proteins, enzymes, and salts were also observed (Gurunathan et al., 2014). In the presence of AgNPs, the catalytic color shift of the dyes was observed visually in Fig. 5. The strength of color steadily decreased over time (Kumari et al., 2016).

This observation is consistent with previous studies (Vanaja et al., 2014; Abd El-Aziz et al., 2018). In conjunction with a previous report, our conclusions were that the best percentage of safranin-dye decline occurred after 72 h, while degradation efficiency was at most at 84.6% (Vanaja et al., 2014). Sorption on the AgNPs surfaces may have caused the deterioration (Kim and Carraway, 2000). Ag NPs depend on their type and scale. Catalytic function. (Switzerland, 2016; Sen, 2014). A huge surface-to - volume ratio is presented to present a significant catalytic activity (Daniel and Astruc, 2003). The degradation in solution of saffron dye red was due to AgNPs lowering the saffron dye. As the AgNP is reduced in size and the number of Ag atoms increases, making it easier to adsorb the catalyst's surface with saffron dye and supporting similar effects (Vidhu and Philip 2013; Bhakya et al., 2015) AgNPs synthesizing through the use of Terminalia chebula fruit extract and their catalytic effect on the reduction of methylene blue have also been reported.

The increase in the concentration of coloring contributes to the degradation of colouring. The degradation rate is directly related to the formation of hydroxy radicals (OH) on the catalyst surface and the possibility that these radicals will react with coloring molasses (Nagar and Devra, 2019). As the concentration of color increases, the generation of OH radicals on the catalyst surface is reduced

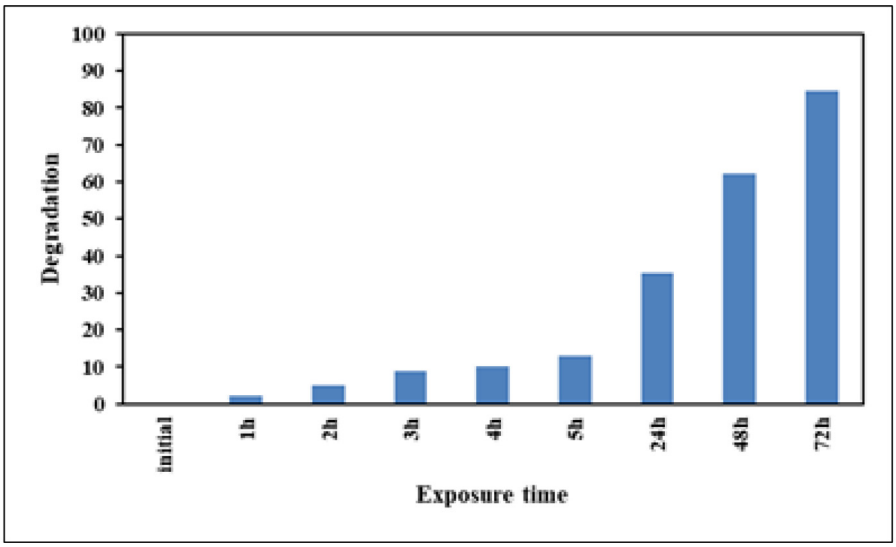

Fig. 7. Percentage of safranin degradation by 10 mg/L of synthesized AgNPs using *S. costus* at different time points.

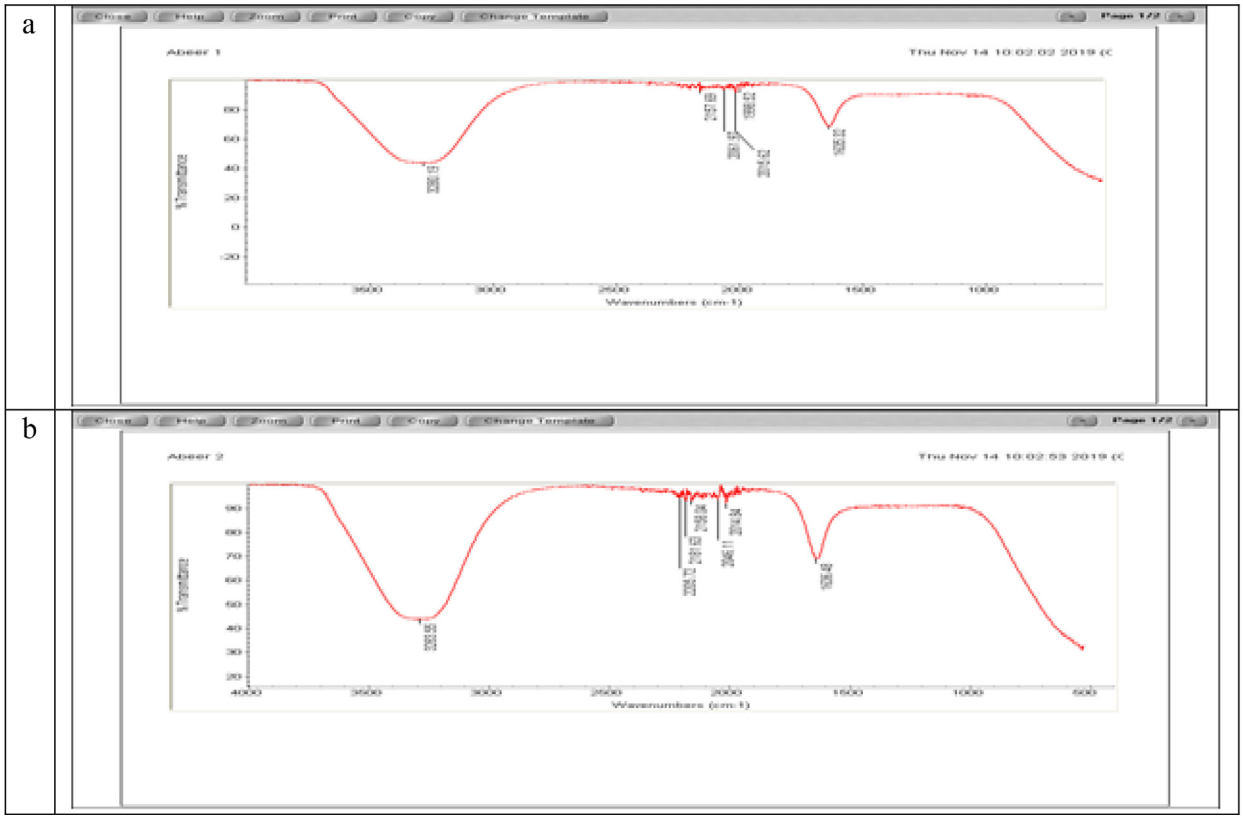

Fig. 8. FTIR spectrum of AgNPs synthesized using *S. costus* root aqueous extract (a) and safranin dye treated with AgNPs (b).

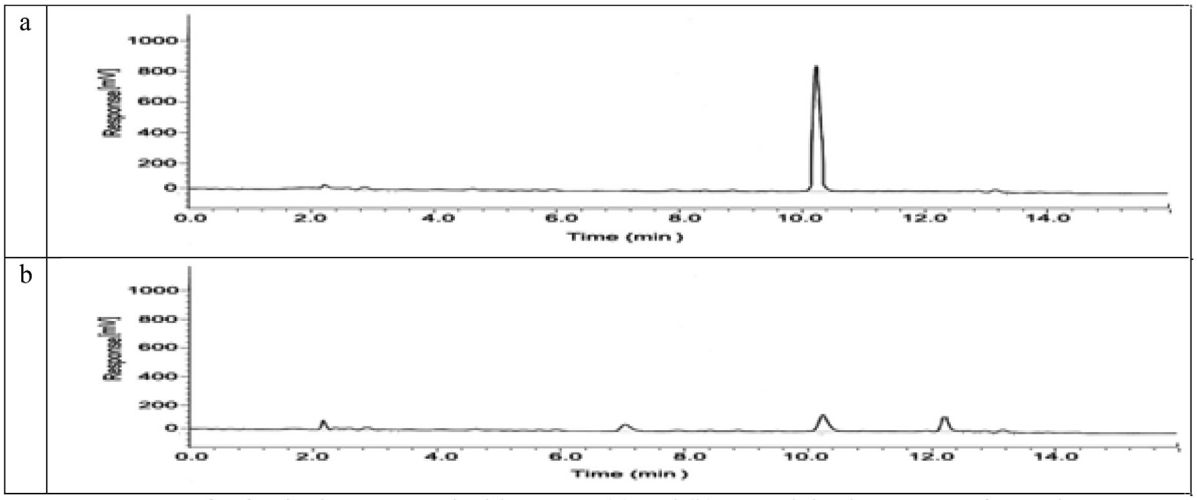

Fig. 9. HPLC of safranin dye untreated with AgNPs (a) and (b) treated dye by AgNPs after 72 h.

because the active locations are also covering with color ions and the photocatalyst surface has less photon, resulting in slow hydroxyl radials output (Tang and An, 1995, Kuma et al., 2008). In addition, when the catalyst is increased to the highest concentration (120 mg L^{-1}), the degradation value has been increased because the amount of adsorptions available and the catalysts available on TiO_2 have been increased. The decoloration rate decreases as a result of an increase in suspension turbidity when TiO_2 dosage has increased above the limiting value (Kuma et al., 2008; El-Kemary et al., 2011).

Degradation caused by increased catalyst migration of the holes on the corresponding surface into the AgNP surface (Ansari et al., 2013). There was a deterioration in the metals surface area, so improving the surface area availability would improve the efficiency of the catalyst. Decreasing particle size will increase catalytic activity, but a substantial dimension below indicates that further declines will interfere with the reaction (Grogger et al., 2004). The electrons transferred from a donor to an accepter are helped with metal nanoparticles (Christopher et al., 2011).

The peak expansion observed was due to the formation of degradation products with a somewhat shifted absorbent band superimposed on carbonyl and aromatic compound functional groups (Segal-Rosenheimer, & Dubowski, 2008). The increase in absorption intensity by 1636,48 cm^1 and 3283,53 cm^1 may be caused by the Quinone or phenol oxidation of aromatic rings (Sibanda et al., 2011).

The results of HPLC agreement with the findings (Lade et al., 2015; Atique Ullah et al., 2017; Bankolea et al., 2018) confirms biodegradation by the decrease in the control color peak and the introduction of several new peaks at the sample with varying retention periods in the treatments, compared to the untreated color with the same peak.

Declaration of Competing Interest

The authors declare that they have no known competing financial interests or personal relationships that could have appeared to influence the work reported in this paper.

Acknowledgments

The authors would like to extend their sincere appreciation to the Deanship of Scientific Research at King Saud University, Kingdom of Saudi Arabia, for funding the research group (RGP-1441-269).

References

Abd El-Aziz, A.R., Al-Othman, M.R., Mahmoud, M.A., 2018. Degradation of DDT by gold nanoparticles synthesized using Lawsonia inermis for environmental safety. Biotechnol. Biotechnol. Equip. 32, 1174–1182.

AL-Mashhedy, L., Al-Kawaz, H.S., 2016. Green Synthesis of Silver Nanoparticles Using Actinidia deliciosa Extracts. Res. J. Pharm., Biol. Chem. Sci. 7, 2212.

Alothman, M., Abd-El-Aziz, A.R.M., 2019. Effect of green synthesis silver nanoparticles from five fruits peel on protein capped and anti-fungal properties. Int. J. Adv. Res. Biol. Sci. 6 (2), 156–165.

Al-Othman, M.R., Abd El-Aziz, A.R.M., Mahmoud, M.A., Ashraf, H.A., 2017. Green biosynthesis of silver nanoparticles using pomegranate peel and inhibitory effects of the nanoparticles on aflatoxin production. Pak. J. Bot. 49 (2), 751–756.

Ansari, S.A., Khan, M.M., Ansari, M.O., Lee, J., Cho, M.H., 2013. Biogenic synthesis, photocatalytic, and photoelectrochemical performance of Ag–ZnO nanocomposite. J. Phys. Chem. C. 117, 27023–27030. https://doi.org/10.1021/jp410063p.

Atique Ullah, A.K.M., Fazle Kibria, A.K.M., Akter, M., Khan, M.N.I., Tareq, A.R.M., Firoz, S.H., 2017. Oxidative Degradation of Methylene Blue Using Mn3O4 Nanoparticles. Water Conser. Sci. Eng. 1, 249–256. https://doi.org/10.1007/s41101-017-0017-3.

Bankolea, P.O., Adekunle, A.A., Govindwar, S., 2018. Enhanced decolorization and biodegradation of acid red 88 dye by newly isolated fungus, *Achaetomium strumarium*. J. Enviro. Chem. Eng. 6, 1589–1600. https://doi.org/10.1016/j.jece.2018.01.069.

Bhakya, S., Muthukrishnan, S., Sukumaran, M., Muthukumar, M., 2015. Catalytic degradation of organic dyes using synthesized silver nanoparticles: A Green Approach. J. Bioremed. Biodeg. 6 (5), 1000312. https://doi.org/10.4172/2155-6199.1000312.

Bonnia, N.N., Kamaruddin, M.S., Nawawi, M.H., Ratim, S., 2016. Green biosynthesis of silver nanoparticles using 'polygonum hydropiper' and study its catalytic degradation of methylene blue. Procedia Chem. 19, 594. https://doi.org/10.1016/j.proche.2016.03.058.

Cariasa, C.C., Novaisa, J.M., Martins-Dias, S., 2008. Are phragmites australis enzymes involved in the degradation of textile azo dye acid orange 7 in a constructed wetland. Biores. Technol. 99, 243. https://doi.org/10.1016/j.biortech.2006.12.034.

Chen, S., Webster, S., Czerw, R., Xu, J., Carroll, D.L., 2004. Morphology effects on the optical properties of silver nanoparticles. Nano Sci. Nanotechnol. 4, 254–259. https://doi.org/10.1166/jnn.2004.034.

Christopher, P., Xin, H., Linic, S., 2011. Visible-light-enhanced catalytic oxidation reactions on plasmonic silver nanostructures. Nat. Chem. 3, 467–472. https://doi.org/10.1038/nchem.1032.

Daniel, M.C., Astruc, D., 2003. Gold nanoparticles: assembly, supramolecular Chemistry, quantum-size-related properties, and applications toward biology, catalysis, and nanotechnology. Chem. Rev. 104, 293–346. https://doi.org/10.1021/cr030698+.

El-Kemary, M., Abdel-Moneam, Y., Madkour, M., El-Mehasseb, I., 2011. Enhanced photocatalytic degradation of Safranin-Obyheterogeneous nanoparticles for environmental applications. J. Lumin. 131, 570–576. https://doi.org/10.1016/j.jlumin.2010.10.025.

Gardea-Torresdey, J.L., Gomez, E., Peralta-Videa, J.R., Jason, G., Troiani, P.H., Jose-Yacaman, M., 2003. Alfalfa sprouts: a natural source for the synthesis of silver nanoparticles. Langmuir 19, 1357–1361. https://doi.org/10.1021/la020835i.

Govindaraju, K., Tamilselvan, S., Kiruthiga, V., Singaravelu, G., 2010. Biogenic silver nanoparticles by Solanum torvum and their promising antimicrobial activity. J. Biopestic. 3, 394–399.

Grogger, C., Fattakhov, S.G., Jouikov, V.V., Shulaeva, M.M., 2004. Primary steps of oxidation and electronic interactions in anodic cleavage of α, ω-diisocyanurate substituted dialkyl disulfides. Electrochim. Acta. 49, 3185–3194.

Gurunathan, B., Bathrinarayanan, P.V., Muthukumarasamy, V.K., Thangavelu, D., 2014. Characterization of intracellular gold nanoparticles synthesized by biomass of Aspergillus terreus. Acta Metall. Sin. Engl. 2014 (27), 569–572. https://doi.org/10.1016/j.electacta.2004.02.032.

Hammami, S., Oturan, N., Bellakhal, N., Oturan, M., 2007. Oxidative degradation of direct orange 61 by electro-fenton process using a carbon felt electrode: application of the experimental design methodology. J. Electroanal. Chern. 610, 75. https://doi.org/10.1016/j.jelechem.2007.07.004.

Hodak, J.H., Martini, I., Hartland, G.V., 1998. Spectroscopy and dynamics of nanometer-sized noble metal particles. J. Phys. Chern. B. 102, 6958. https://doi.org/10.1021/jp9809787.

Jadhava, U.U., Dawkara, V.V., Ghodakea, G.S., Govindwar, S.P., 2008. Biodegradation of Direct Red 5B, a textile dye by newly isolated Comamonas sp. UVSJ. Hazard. Mater. 158, 507–516. https://doi.org/10.1016/j.jhazmat.2008.01.099.

Kim, Y.H., Carraway, E.R., 2000. Dechlorination of pentachlorophenol by zero valent iron and modified zero valent irons. Environ. Sci. Technol. 34, 2014–2017. https://doi.org/10.1021/es991129f.

Kuma, P., Sivakumar, R., Anandan, S., Madhavan, J., Maruthamuthu, P., Ashokkumar, M., 2008. Photocatalytic degradation of acid red 88 using Au–TiO2 nanoparticles in aqueous solutions. Water Res. 42, 4878–4884. https://doi.org/10.1016/j.watres.2008.09.027.

Kumari, M.R., Thapa, N., Gupta, N., Kumar, A., Nimesh, S., 2016. Antibacterial and photocatalytic degradation efficacy of silver nanoparticles biosynthesized using Cordia dichotoma leaf extract. Adv. Nat. Sci.-Nanosci. 7, 045009.

Lade, H., Govindwar, S., Paul, D., 2015. Mineralization and detoxification of the carcinogenic azo dye congo red and real textile effluent by a polyurethane foam immobilized microbial consortium in an upflow column bioreactor. Int. J. Environ. Res. Public Health. 12, 6894–6918. https://doi.org/10.3390/ijerph120606894.

Liu, G., Zhao, J., 2000. Photocatalytic degradation of dye sulforhodamine B: a comparative study of photocatalysis with photosensitization. New J. Chern. 24, 411. https://doi.org/10.1039/B001573N.

Logunov, S.L., Ahmadi, T.S., El Sayd, M.A., Khoury, J.T., 1997. Whetten, R.L. Electron dynamics of passivated gold nanocrystals probed by subpicosecond transient absorption spectroscopy. J. Phys. Chern. B, 101, 3713. https://doi.org/10.1021/jp962923f.

Mahapatra, D.K., Tijare, L.K., Gundimeda, V., Mahajan, N., 2018. Rapid Biosynthesis of Silver Nanoparticles of Flower-like Morphology from the Root Extract of Saussurea lappa. Res. Rev. J. Pharm. Pharmacogn. Res. 5, 1, 20–24.

Nagar, N., Devra, V., 2019. A kinetic study on the degradation and biodegradability of silver nanoparticles catalyzed Methyl Orange and textile effluents. Heliyon. 5,. https://doi.org/10.1016/j.heliyon.2019.e01356 e01356.

Rao, M.L., Savithramma, N., 2011. Biological synthesis of silver nanoparticles using svensonia hyderabadensis leaf extract and evaluation of their antimicrobial efficacy. Int. J. Innov. Pharm. Sci. Res. 3, 1117–1121.

Ravindran, A., Chandran, P., 2013. Biofunctionalized silver nanoparticles: advances and prospects. Colloids Surf. B. 105, 342. https://doi.org/10.1016/j.colsurfb.2012.07.036.

Saxena, A., Tripathi, R.M., Zafar, F., Singh, P., 2012. Green synthesis of silver nanoparticles using aqueous solution of Ficus benghalensis leaf extract and characterization of their antibacterial activity. Mater. Lett. 67, 91. https://doi.org/10.1016/j.matlet.2011.09.038.

Segal-Rosenheimer, M., Dubowski, Y., 2008. Photolysis of thin films of cypermethrin using in situ FTIR monitoring: products, rates and quantum yields. J. Photochem Photobiol. A. 200, 262–269. https://doi.org/10.1016/j.jphotochem.2008.08.004.

Sibanda, M.M., Focke, W.W., Labuschagne, F.J., Moyo, L., Nhlapo, N.S., Maity, A., Muiambo, H., Massinga, P., Crowther, N.A., Coetzee, M., Brindley, G.W., 2011. Degradation of insecticides used for indoor spraying in malaria control and possible solutions. Malaria J. 10, 307. https://doi.org/10.1186/1475-2875-10.

Tang, W.Z., An, H., 1995. UV-TiO2 photocatalytic oxidation of commercial dyesin aqueous solutions. Chemosphere. 31, 4157–4170. https://doi.org/10.1016/0045-6535(95)80015-D.

Vanaja, M.K., Paulkumar, M., Baburaja, S., Rajeshkumar, S., Gnanajobitha, G., Malarkodi, C., Sivakavinesan, M., Annadurai, G., 2014. Degradation of methylene blue using biologically synthesized silver Nanoparticles. Bioinorg. Chem. Appl. 2014,. https://doi.org/10.1155/2014/742346 742346.

Vidhu, V.K., Philip, D., 2013. Catalytic degradation of organic dyes using biosynthesized silver nanoparticles. Micron. 56, 54–62. https://doi.org/10.1016/j.micron.2013.10.006.

Vinodgopal, K., Kamat, P.V., 1995. Enhanced rates of photocatalytic degradation of an Azo dye using SnO2/TiO_2 Coupled semiconductor thin films. Environ. Sci. Technol. 29, 841. https://doi.org/10.1021/es00003a037.